

# Generalized Gouy phase for focused partially coherent light and its implications for interferometry

Xiaoyan Pang,<sup>1</sup> David G. Fischer,<sup>2</sup> and Taco D. Visser<sup>1,3,\*</sup>

<sup>1</sup>*Department of Electrical Engineering, Delft University of Technology, Delft, The Netherlands*

<sup>2</sup>*Research and Technology Directorate, NASA Glenn Research Center, Cleveland, Ohio 44135, USA*

<sup>3</sup>*Department of Physics and Astronomy, VU University, Amsterdam, The Netherlands*

\**Corresponding author: T.D.Visser@tudelft.nl*

Received March 16, 2012; accepted March 27, 2012;

posted March 30, 2012 (Doc. ID 164864); published May 23, 2012

The Gouy phase, sometimes called the phase anomaly, is the remarkable effect that in the region of focus a converging wave field undergoes a rapid phase change by an amount of  $\pi$ , compared to the phase of a plane wave of the same frequency. This phenomenon plays a crucial role in any application where fields are focused, such as optical coherence tomography, mode selection in laser resonators, and interference microscopy. However, when the field is spatially partially coherent, as is often the case, its phase is a random quantity. When such a field is focused, the Gouy phase is therefore undefined. The correlation properties of partially coherent fields are described by their so-called spectral degree of coherence. We demonstrate that this coherence function *does* exhibit a generalized Gouy phase. Its precise behavior in the focal region depends on the transverse coherence length. We show that this effect influences the fringe spacing in interference experiments in a nontrivial manner. © 2012 Optical Society of America

OCIS codes: 030.1640, 050.1960, 180.3170, 120.3940.

In 1890 Gouy found that the phase of a monochromatic, diffracted converging wave, compared to that of a plane wave of the same frequency, undergoes a rapid change of  $180^\circ$  near the geometrical focus [1–4]. Since then many further observations of this so-called *phase anomaly* have been reported and many different explanations for its origin have been suggested (see [5] and the references therein). The Gouy phase is of great importance because of its role in, for example, metrology [6], laser mode conversion [7], coherence tomography [8], the tuning of laser cavities [9], higher order harmonic generation [10], terahertz time-domain spectroscopy [11], and nanooptics [12].

Under many practical circumstances, light is not monochromatic, but rather partially coherent. Examples are light that is produced by a multimode laser or light that has traveled through the atmosphere or biological tissue. In those cases, the phase of the wave field is a random quantity. Therefore, when a partially coherent field is focused (as described in [13–20]), the Gouy phase is undefined; i.e., it has no physical meaning. In the space-frequency domain, a partially coherent optical field is characterized by two-point correlation functions, such as the cross-spectral density or its normalized version, the spectral degree of coherence [21]. These complex-valued functions have a phase that is typically well-defined. As we will demonstrate for a broad class of partially coherent fields, the phase of both correlation functions shows a generalized phase anomaly, which reduces to the classical Gouy phase in the coherent limit. Furthermore, this generalized Gouy phase affects the interference of highly focused fields, in microscopy for example, altering the fringe spacing compared to that of a coherent field.

Consider first a converging, monochromatic field of frequency  $\omega$  that is exiting a circular aperture with radius  $a$

in a plane screen (see Fig. 1). The origin  $O$  of the coordinate system coincides with the geometrical focus. The amplitude of the field is  $U^{(0)}(\mathbf{r}', \omega)$ ,  $\mathbf{r}'$  being the position vector of a point  $Q$  in the aperture. The field at a point  $P(\mathbf{r})$  in the focal region is, according to the Huygens–Fresnel principle [4, Chap. 8.2], given by the following expression:

$$U(\mathbf{r}, \omega) = -\frac{i}{\lambda} \int_s U^{(0)}(\mathbf{r}', \omega) \frac{\exp(iks)}{s} d^2r', \quad (1)$$

where the integration extends over the spherical wave front  $S$  that fills the aperture,  $s = |\mathbf{r} - \mathbf{r}'|$  denotes the distance  $QP$ , and  $k = 2\pi/\lambda$  is the wavenumber associated with frequency  $\omega$ . A periodic time-dependent factor  $\exp(-i\omega t)$  is suppressed.

The Gouy phase  $\delta(z)$  of a focused, monochromatic field at an axial point  $\mathbf{r} = (0, 0, z)$  is defined as the difference between the argument (or “phase”) of the field  $U(z, \omega)$  and that of a plane wave (or a spherical wave) of the same frequency, i.e.,

$$\delta(z) = \arg[U(z, \omega)] - kz. \quad (2)$$

One can show that [4, Sec. 8.8.4]

$$\delta(0) = -\pi/2. \quad (3)$$

Furthermore, the Gouy phase has the symmetry property

$$\delta(z) + \delta(-z) = -\pi. \quad (4)$$

An example of the behavior of the Gouy phase near focus is shown in Fig. 2. The discontinuities by an amount of  $\pi$  occur at the zeros (or phase singularities) of the field. The slope of the curve through the point  $z = 0$  is explained by the observation

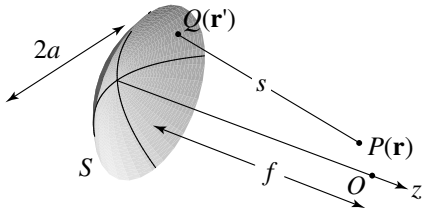


Fig. 1. Illustration of the notation.

by Linfoot and Wolf [3] that near focus the wavefronts are separated by a distance  $\lambda/(1 - a^2/4f^2)$ . This implies that the effective phase of the field, compared to that of a plane wave, lags by an amount of  $kza^2/4f^2$ . For the choice of parameters in Fig. 2 this translates into a slope of  $-0.621$  radians per micrometer, as is indeed observed.

For a partially coherent wave field one must consider, instead of the amplitude  $U^{(0)}(\mathbf{r}, \omega)$ , the *cross-spectral density function* [21, Sec. 2.4.4] of the field at two points  $Q_1(\mathbf{r}'_1)$  and  $Q_2(\mathbf{r}'_2)$ , namely,

$$W^{(0)}(\mathbf{r}'_1, \mathbf{r}'_2, \omega) = \langle U^{(0)*}(\mathbf{r}'_1, \omega)U^{(0)}(\mathbf{r}'_2, \omega) \rangle. \quad (5)$$

Here the angular brackets denote the average, taken over a statistical ensemble of monochromatic realizations  $\{U^{(0)}(\mathbf{r}') \exp(-i\omega t)\}$  [21, Sec. 4.7] and the asterisk denotes the complex conjugate. The cross-spectral density of the focused field

$$W(\mathbf{r}_1, \mathbf{r}_2, \omega) = \langle U^*(\mathbf{r}_1, \omega)U(\mathbf{r}_2, \omega) \rangle \quad (6)$$

is, according to Eqs. (1) and (6), given by the following formula:

$$W(\mathbf{r}_1, \mathbf{r}_2, \omega) = \frac{1}{\lambda^2} \iint_S \iint_S W^{(0)}(\mathbf{r}', \mathbf{r}'', \omega) \times \frac{\exp[ik(s_2 - s_1)]}{s_1 s_2} d^2r' d^2r'', \quad (7)$$

where  $s_1 = |\mathbf{r}_1 - \mathbf{r}'|$ , and  $s_2 = |\mathbf{r}_2 - \mathbf{r}''|$ . To simplify the notation, we omit the dependence of the various quantities on the frequency  $\omega$  from now on.

We assume that the field in the aperture is a Gaussian Schell-model field with uniform intensity  $A^2$  [21, Sec. 5.3.2]; i.e.,

$$W^{(0)}(\mathbf{r}', \mathbf{r}'') = W^{(0)}(\rho', \rho'') \quad (8)$$

$$= A^2 \exp[-(\rho'' - \rho')^2/2\sigma^2], \quad (9)$$

where  $\rho = (x, y)$  is the two-dimensional transverse vector that specifies the position of a point  $Q$  on  $S$  and  $\sigma$  is a positive

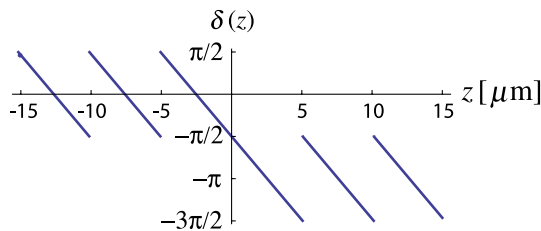


Fig. 2. (Color online) Classical Gouy phase  $\delta(z)$  along the optical axis for a deterministic (i.e., fully coherent) wave field. In this example,  $a = 1$  cm,  $f = 2$  cm, and  $\lambda = 0.6328$   $\mu\text{m}$ .

constant indicating the effective transverse spectral coherence length of the field.

A normalized measure of the strength of the field correlations at a pair of points  $P_1(\mathbf{r}_1), P_2(\mathbf{r}_2)$  in the focal region is given by the *spectral degree of coherence* [21, Sec. 4.3.2], which is defined as

$$\mu(\mathbf{r}_1, \mathbf{r}_2) = \frac{W(\mathbf{r}_1, \mathbf{r}_2)}{\sqrt{S(\mathbf{r}_1)S(\mathbf{r}_2)}}, \quad (10)$$

with the *spectral density* (“intensity at frequency  $\omega$ ”)  $S(\mathbf{r}_i)$  at position  $\mathbf{r}_i$  given by the diagonal elements of the cross-spectral density, i.e.,

$$S(\mathbf{r}_i) = W(\mathbf{r}_i, \mathbf{r}_i), \quad i = 1, 2. \quad (11)$$

Because  $S(\mathbf{r}_i)$  is real-valued and never zero for Gaussian Schell-model fields [16], the arguments (or “phases”) of the spectral degree of coherence and that of the cross-spectral density function are identical.

We restrict our analysis to pairs of points on the  $z$  axis, i.e.,  $\mathbf{r}_1 = (0, 0, z_1), \mathbf{r}_2 = (0, 0, z_2)$ . On making use of the Debye approximation [4, Sec. 8.8.1], one can then derive for the cross-spectral density the following expression (see [22] for details):

$$W(z_1, z_2) = \left(\frac{2\pi A}{\lambda f}\right)^2 \int_0^a \int_0^a \exp[-(\rho^2 + \rho'^2)/2\sigma^2] \times \exp\{ik[-z_1(1 - \rho^2/2f^2) + z_2(1 - \rho'^2/2f^2)]\} \times I_0\left(\frac{\rho'\rho''}{\sigma^2}\right) \rho'\rho'' d\rho' d\rho'', \quad (12)$$

where  $I_0$  denotes the modified Bessel function of order zero.

Let us now define a *generalized Gouy phase* as

$$\delta_\mu(z_1, z_2) = \arg[W(z_1, z_2)] + kz_1 - kz_2. \quad (13)$$

Here the subscript  $\mu$  indicates that this definition pertains to the phase of the correlation functions, i.e., that of the spectral degree of coherence or, equivalently, that of the cross-spectral density. The reference phases  $kz_1$  and  $kz_2$  are those of a plane wave of frequency  $\omega = kc$ , with  $c$  the speed of light, at positions  $z_1$  and  $z_2$ , respectively. In contrast to the classical Gouy phase, definition (13) involves the phase of a two-point correlation function rather than that of a deterministic wave field that only depends on a single spatial variable. In addition, two reference phases are taken into account instead of one.

Let us take the first observation point at the origin  $O$ ; i.e.,  $z_1 = 0$ . Then Eq. (12) reduces to

$$\delta_\mu(0, z_2) = \arg \left[ \int_0^a \int_0^a \exp[-(\rho^2 + \rho'^2)/2\sigma^2] \times \exp\{-ik[z_2\rho'^2/2f^2]\} \times I_0\left(\frac{\rho'\rho''}{\sigma^2}\right) \rho'\rho'' d\rho' d\rho'' \right]. \quad (14)$$

Examples of the generalized Gouy phase are shown in Fig. 3 for different values of the transverse coherence length  $\sigma$ . It is seen that  $\delta_\mu(0, z_2)$  exhibits an anomalous phase behavior that is quite similar to that of deterministic fields, with the phase near focus undergoing a rapid phase change of  $\pi$ . In addition, the generalized Gouy phase obeys the following relations:

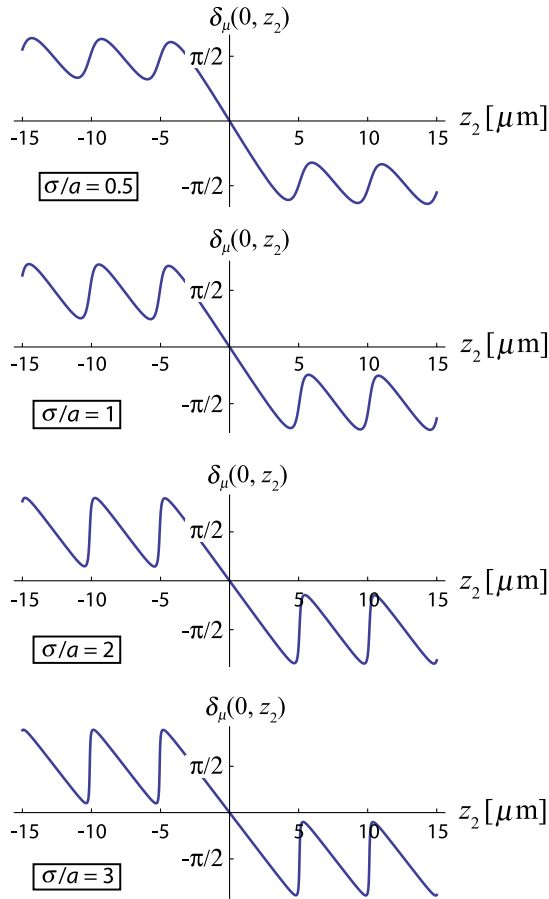


Fig. 3. (Color online) Generalized Gouy phase  $\delta_\mu(0, z_2)$  of a partially coherent field for different values of the transverse coherence length of the field in the aperture, namely,  $\sigma = 0.5$  cm 1, 2, and 3 cm. In all examples, the aperture radius  $a = 1$  cm, the focal length  $f = 2$  cm, and the wavelength  $\lambda = 0.6328$   $\mu\text{m}$ .

$$\delta_\mu(0, 0) = 0, \quad (15)$$

$$\delta_\mu(0, z_2) + \delta_\mu(0, -z_2) = 0, \quad (16)$$

which are the statistical analogs of Eqs. (3) and (4) for the deterministic case. In fact, apart from a  $\pi/2$  offset, which can be traced back to the prefactor  $i$  in Eq. (1), they are identical.

On the other hand, there are some striking differences. For instance, the modulation depth of the generalized Gouy phase is dependent on the transverse coherence length of the incident field. It is small for incoherent fields and increases in size as the coherence length is increased. In addition, the generalized Gouy phase has regions of both positive and negative slope, unlike the coherent case for which the slope is always negative. The implications of this for interference experiments will be discussed shortly.

That the classical phase anomaly is a special case of the generalized Gouy phase follows from consideration of a deterministic wave field. For such a field, the ensemble average reduces to a single realization, and the cross-spectral density of Eq. (6) factorizes into the form

$$W(z_1, z_2) = U^*(z_1)U(z_2). \quad (17)$$

On making use of Eqs. (3) and (17) and setting  $z_1 = 0$ , we see that the generalized Gouy phase Eq. (13) reduces to

$$\delta_\mu(0, z_2) = \arg[U(z_2)] - kz_2 + \pi/2, \quad (18)$$

which is, apart from an inconsequential constant, the classical definition, Eq. (2). Furthermore, in the coherent limit ( $\sigma \rightarrow \infty$ ) Eq. (14) can be solved analytically and we obtain the result that near  $z = 0$

$$\delta_\mu(0, z_2) = -kz_2 a^2 / 4f^2, \quad (19)$$

which is identical to the Gouy phase behavior of deterministic waves as discussed in connection with Fig. 2. In [5] it was discussed how the physical origin of the classical Gouy phase can be explained by a stationary phase argument. A similar explanation holds for the generalized Gouy phase.

It is well known that the fringe spacing in interference microscopy is typically irregular, and it depends on both the numerical aperture (NA) and the apodization [23,24]. It has also recently been established that the spatial coherence of the incident field plays a role, although its treatment has been empirical to date. To quantitatively investigate the effects of spatial coherence on interference fringe spacing (and, ultimately, on interference metrology) and the role that the generalized Gouy phase plays, we consider the Linnik microscope [6]. In such a two-beam configuration, the fields at two different positions along the  $z$  axis are combined, producing a fringe pattern (“interferogram”). On making use of Eq. (10) we can write the spectral density of this superposition as

$$I(z) = |U(0) + U(z)|^2, \quad (20)$$

$$= S(0) + S(z) + 2\sqrt{S(0)S(z)} \text{Re}[\mu(0, z)], \quad (21)$$

which is commonly known as the “spectral interference law” [21, Sec. 4.3]. It is clear from Eq. (21) that for an interferogram, in which the spectral density of the superposition is recorded as a function of the distance  $z$ , the spacing of the ensuing fringes is determined by both  $S(z)$ , the spectral density, and  $\mu(0, z)$ , the spectral degree of coherence of the field. In our model, the latter is characterized by a single parameter, namely the transverse coherence length  $\sigma$  of the field in the aperture. As was seen in Fig. 3, this parameter has a significant influence on the phase behavior of the spectral degree of coherence near focus.

For low-NA fields,  $S(z)$  is a slowly varying function compared to  $\mu(0, z)$ , which varies sinusoidally on the scale of the wavelength. For high-NA fields, however,  $S(z)$  changes much faster and the maxima of the interference term in Eq. (21) are no longer coincident with those of  $\text{Re}[\mu(0, z)]$ .

To quantify the effect of the state of coherence of the incident field on the interference process, we have computed the spacing of the fringes for three cases, each with the same (relatively high) NA and varying degrees of spatial coherence:  $\sigma/a = 0.5$ ,  $\sigma/a = 1$ , and  $\sigma/a = 50$ . The results are listed in Table 1 for the first 11 fringes. As can be seen, in all three cases, the spacings of the first several fringes, which are primarily dictated by  $\mu(0, z)$ , are larger than the free-space wavelength. This increased spacing was discussed earlier for the coherent case, and it is due to the behavior of the Gouy

**Table 1. Fringe Spacings for Three Values of the Transverse Coherence Length  $\sigma^a$** 

#	$\sigma/a = 0.5$	$\sigma/a = 1$	$\sigma/a = 50$
1	0.6675	0.6702	0.6730
2	0.6671	0.6699	0.6730
3	0.6662	0.6695	0.6730
4	0.6642	0.6683	0.6729
5	0.6602	0.6657	0.6724
6	0.6509	0.6582	0.6702
7	0.6284	0.6311	0.6560
8	0.5944	0.5579	0.4647
9	0.6044	0.5926	0.5975
10	0.6368	0.6465	0.6652
11	0.6519	0.6601	0.6704

<sup>a</sup>In all cases, the aperture radius  $a = 1$  cm, the focal length  $f = 2$  cm, and the free-space wavelength  $\lambda = 0.6328 \mu\text{m}$ .

phase. Accordingly, if the fringe spacings were due solely to  $\mu(0, z)$ , in the coherent case we would expect them to be identical except when the region between the corresponding intensity maxima contains a phase discontinuity of the Gouy phase. That this is not the case is due to the fact that the spectral density  $S(z)$  modulates the spectral degree of coherence [in Eq. (21)] and displaces additional maxima in the neighborhood of the discontinuities. By contrast, for the partially coherent cases, a greater number of fringes are inherently affected near the phase jumps of the generalized Gouy phase. This is because the transition at the jumps is more gradual (i.e., not a true discontinuity). Furthermore, as the field becomes less coherent, the size of the jumps (i.e., the modulation depth) decreases and the transition near the jumps becomes smoother. Therefore, the fringe spacing is highly irregular in all three cases, with the maximum fringe displacement (#8) occurring for the coherent case ( $\sigma/a = 50$ ) and the maximum fringe variation (greater number of affected fringes) and smallest fringe displacement occurring for the least coherent case. The maximum fringe displacements, given by the eighth fringe in each case, are 0.5944, 0.5579, and 0.4647, from least coherent to most coherent. In Figs. 4 and 5, we have plotted the interferograms corresponding to the first and third cases in Table 1 ( $\sigma/a = 0.5$  and  $\sigma/a = 50$ ). It is seen in Fig. 4 that the fringe spacing of the fully coherent field (dashed red curve) is initially somewhat larger than that of the partially coherent field (solid blue curve). However, Fig. 5 shows that for larger values of  $z_2$  the fringes of the fully coherent field move closer together and the maxima of the

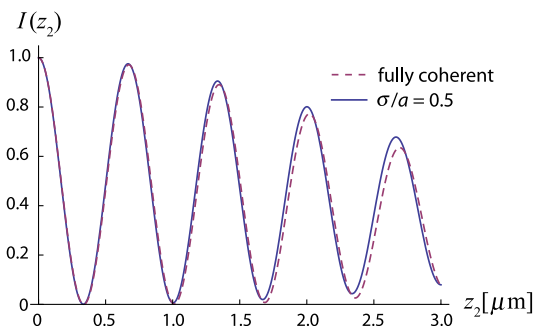


Fig. 4. (Color online) Interferogram for a coherent field ( $\sigma/a = 50$ ) (dashed red curve) and for a partially coherent field ( $\sigma/a = 0.5$ ) (solid blue curve). In both cases,  $a = 1$  cm,  $f = 2$  cm and  $\lambda = 0.6328 \mu\text{m}$ .

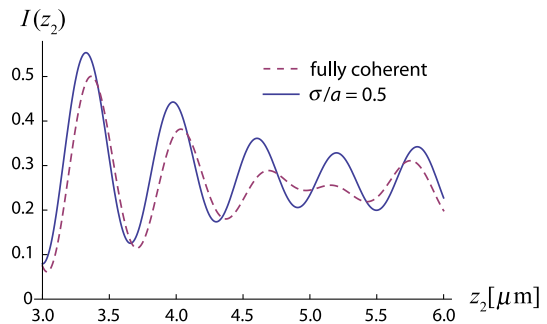


Fig. 5. (Color online) Same as Fig. 4, but for larger values of the axial position  $z_2$ .

fringe pattern go from trailing the partially coherent case to leading it. This transition occurs around  $z_2 = 4.5 \mu\text{m}$ , which is precisely the point where the slope of the generalized Gouy phase changes from being negative to being positive (see the top panel of Fig. 3). Near  $z_2 = 6.0 \mu\text{m}$ , the sign of this slope changes again and the fringe spacing of the partially coherent field again becomes smaller than that of the fully coherent field. The slope of the classical Gouy phase (as shown in Fig. 2) is, apart from the discontinuities at the axial phase singularities, always negative. Therefore, such an effect does not occur for coherent fields.

In conclusion, we have defined a generalized Gouy phase for partially coherent fields. In contrast to its traditional counterpart, this phase pertains to the spectral degree of coherence, a two-point correlation function, rather than to the phase of a deterministic wave field that depends only on a single point. It was shown that the classical phase anomaly is a special case of the generalized Gouy phase. The generalized Gouy phase was examined numerically and analytically for the broad class of Gaussian-correlated fields. It was demonstrated that our findings have important implications for metrology with partially coherent fields.

## REFERENCES

1. L. G. Gouy, "Sur une propriété nouvelle des ondes lumineuses," C.R. Acad. Sci. **110**, 1251–1253 (1890).
2. L. G. Gouy, "Sur la propagation anormale des ondes," Ann. Chim. Phys. **24**, 145–213 (1891).
3. E. H. Linfoot and E. Wolf, "Phase distribution near focus in an aberration-free diffraction image," Proc. Phys. Soc. B **69**, 823–832 (1956).
4. M. Born and E. Wolf, *Principles of Optics*, 7th (expanded) ed. (Cambridge University, 1999).
5. T. D. Visser and E. Wolf, "The origin of the Gouy phase anomaly and its generalization to astigmatic wavefields," Opt. Commun. **283**, 3371–3375 (2010).
6. G. S. Kino and T. R. Korle, *Confocal Scanning Optical Microscopy and Related Imaging Systems* (Academic, 1996).
7. M. W. Beijersbergen, L. Allen, H. E. L. O. van der Veen, and J. P. Woerdman, "Astigmatic laser mode converters and transfer of orbital angular momentum," Opt. Commun. **96**, 123–132 (1993).
8. G. Lamouche, M. L. Dufour, B. Gauthier, and J.-P. Monchalain, "Gouy phase anomaly in optical coherence tomography," Opt. Commun. **239**, 297–301 (2004).
9. T. Klaassen, A. Hoogeboom, M. P. van Exter, and J. P. Woerdman, "Gouy phase of nonparaxial eigenmodes in a folded resonator," J. Opt. Soc. Am. A **21**, 1689–1693 (2004).
10. F. Lindner, W. Stremme, M. G. Schätzel, F. Grasbon, G. G. Paulus, H. Walther, R. Hartmann, and L. Strüder, "High-order harmonic generation at a repetition rate of 100 kHz," Phys. Rev. A **68**, 013814 (2003).

11. J. F. Federici, R. L. Wample, D. Rodriguez, and S. Mukherjee, "Application of terahertz Gouy phase shift from curved surfaces for estimation of crop yield," *Appl. Opt.* **48**, 1382–1388 (2009).
12. M.-S. Kim, T. Scharf, S. Mühlig, C. Rockstuhl, and H. P. Herzig, "Gouy phase anomaly in photonic nanojets," *Appl. Phys. Lett.* **98**, 191114 (2011).
13. W. Wang, A. T. Friberg, and E. Wolf, "Focusing of partially coherent light in systems of large Fresnel number," *J. Opt. Soc. Am. A* **14**, 491–496 (1997).
14. A. T. Friberg, T. D. Visser, W. Wang, and E. Wolf, "Focal shifts of converging diffracted waves of any state of spatial coherence," *Opt. Commun.* **196**, 1–7 (2001).
15. B. Lü, B. Zhang, and B. Cai, "Focusing of a Gaussian Schell-model beam through a circular lens," *J. Mod. Opt.* **42**, 289–298 (1995).
16. T. D. Visser, G. Gbur, and E. Wolf, "Effect of the state of coherence on the three-dimensional spectral intensity distribution near focus," *Opt. Commun.* **213**, 13–19 (2002).
17. G. Gbur and T. D. Visser, "Can coherence effects produce a local minimum of intensity at focus?" *Opt. Lett.* **28**, 1627–1629 (2003).
18. T. van Dijk, G. Gbur, and T. D. Visser, "Shaping the focal intensity distribution using spatial coherence," *J. Opt. Soc. Am. A* **25**, 575–581 (2008).
19. S. B. Raghunathan, T. van Dijk, E. J. G. Peterman, and T. D. Visser, "Experimental demonstration of an intensity minimum at the focus of a laser beam created by spatial coherence: application to the optical trapping of dielectric particles," *Opt. Lett.* **35**, 4166–4168 (2010).
20. G. Gbur and T. D. Visser, "The structure of partially coherent fields," in *Progress in Optics*, Vol. 55, E. Wolf, ed. (Elsevier, 2010), pp. 285–341.
21. L. Mandel and E. Wolf, *Optical Coherence and Quantum Optics* (Cambridge University, 1995).
22. D. G. Fischer and T. D. Visser, "Spatial correlation properties of focused partially coherent light," *J. Opt. Soc. Am. A* **21**, 2097–2102 (2004).
23. J. T. Foley and E. Wolf, "Wave-front spacing in the focal region of high-numerical-aperture systems," *Opt. Lett.* **30**, 1312–1314 (2005).
24. K. Creath, "Calibration of numerical aperture effects in interferometric microscope objectives," *Appl. Opt.* **28**, 3333–3338 (1989).